

**Serveur Académique Lausannois SERVAL [serval.unil.ch](http://serval.unil.ch)**

## **Author Manuscript**

**Faculty of Biology and Medicine Publication**

**This paper has been peer-reviewed but does not include the final publisher proof-corrections or journal pagination.**

Published in final edited form as:

**Title:** Simultaneous coexpression of memory-related and effector-related genes by individual human CD8 T cells depends on antigen specificity and differentiation.

**Authors:** Gupta B, Iancu EM, Gannon PO, Wieckowski S, Baitsch L, Speiser DE, Rufer N

**Journal:** Journal of immunotherapy (Hagerstown, Md. : 1997)

**Year:** 2012 Jul

**Volume:** 35

**Issue:** 6

**Pages:** 488-501

**DOI:** 10.1097/CJI.0b013e31826183a7

In the absence of a copyright statement, users should assume that standard copyright protection applies, unless the article contains an explicit statement to the contrary. In case of doubt, contact the journal publisher to verify the copyright status of an article.

**Simultaneous co-expression of memory- and effector-related genes by individual human CD8 T cells depends on antigen specificity and differentiation**

Bhawna Gupta<sup>1,\*</sup>, Emanuela M. Iancu<sup>1,\*</sup>, Philippe O. Gannon<sup>1,\*</sup>, Sébastien Wieckowski<sup>1</sup>, Lukas Baitsch<sup>2</sup>, Daniel E. Speiser<sup>2</sup> and Nathalie Rufer<sup>1,2</sup>

<sup>1</sup>Department of Research, Lausanne University Hospital, Lausanne, Switzerland

<sup>2</sup>Ludwig Center for Cancer Research, University of Lausanne, Lausanne, Switzerland

\* These authors contributed equally to this work

**Address correspondence to:** Nathalie Rufer, PhD, Department of Research, Lausanne University Hospital, c/o HO, niv 5, Avenue Pierre-Decker 4, CH-1011 Lausanne, Switzerland; [Nathalie.Rufer@unil.ch](mailto:Nathalie.Rufer@unil.ch)

**Running title:** Single T cell gene co-expression profiling

**Keywords:** human, melanoma, vaccination, EBV, CMV, CD8 T cells, single-cell, TCR clonotype, cell differentiation, memory, homing, effector, gene expression

**Abbreviations:** IFA, Incomplete Freund's Adjuvant; EBV, Epstein-Barr virus; CMV, Cytomegalovirus

**Author contributions:** B.G., E.M.I., P.O.G., D.E.S., and N.R. designed research. B.G., E.M.I., P.O.G., S.W., L.B. and N.R. performed research and analyzed data. B.G., P.O.G., D.E.S., and N.R. wrote the manuscript.

**ABSTRACT**

Phenotypic and functional cell properties are usually analyzed at the level of defined cell populations but not single cells. Yet, large differences between individual cells may have important functional consequences. It is likely that T cell mediated immunity depends on the polyfunctionality of individual T cells, rather than the sum of functions of responding T cell subpopulations. We performed highly sensitive single-cell gene expression profiling, allowing the direct *ex vivo* characterization of individual virus- and tumor-specific T cells from healthy donors and melanoma patients. We have previously shown that vaccination with the natural tumor peptide Melan-A<sup>MART-1</sup><sub>26-35</sub> induced T cells with superior effector functions as compared to vaccination with the analog peptide optimized for enhanced HLA-A\*0201 binding. Here we found that natural peptide vaccination induced tumor-reactive CD8<sup>POS</sup> T cells with frequent co-expression of both memory/homing-associated genes (*CD27*, *IL7R*, *EOMES*, *CXCR3* and *CCR5*) and effector-related genes (*IFNG*, *KLRD1*, *PRF1*, and *GZMB*), comparable to protective EBV- and CMV-specific T cells. In contrast, memory/homing- and effector-associated genes were less frequently co-expressed after vaccination with the analog peptide. Remarkably, these findings reveal a previously unknown level of gene expression diversity among vaccine- and virus-specific T cells with the simultaneous co-expression of multiple memory/homing- and effector-related genes by the same cell. Such broad functional gene expression signatures within antigen-specific T cells may be critical for mounting efficient responses to pathogens or tumors. In summary, direct *ex vivo* high-resolution molecular characterization of individual T cells provides key insights into the processes shaping the functional properties of tumor- and virus-specific T cells.

## INTRODUCTION

Analysis of the generation, function and long-term persistence of effector and memory T lymphocytes has been of fundamental importance to our understanding of protective immunity and to improve therapeutic vaccine strategies. Following TCR triggering, naive T cell precursors differentiate into antigen-experienced CD8<sup>POS</sup> T lymphocytes, forming highly heterogeneous memory- and effector-like subpopulations based on their phenotype, function and anatomic location.<sup>1-3</sup> During T cell differentiation, stochastic events involve a set of modifications of multiple gene expressions inducing drastic changes in the cell and thus sustaining variability among the antigen-primed subpopulations. A powerful approach to explore the biological basis underlying differentiation of memory- and effector-like T cell subsets relies on molecular gene signature analyses using DNA microarrays. For instance, gene expression profiling led to the identification of memory- and effector-associated gene expression markers defining distinct functional properties of memory progenitor and terminal effector CD8<sup>POS</sup> T cells,<sup>4-6</sup> and provided new insights in the progressive generation of those subsets during acute viral infection.<sup>7,8</sup> Genome-wide analysis further revealed a gene expression program diversion between CD4<sup>POS</sup> and CD8<sup>POS</sup> T cells at early stages of differentiation, contrasting with the similar molecular profiles found as cells reach later differentiation stages.<sup>9</sup> Moreover, functional cell exhaustion was associated with numerous molecular alterations in virus-specific T cells from chronic infections,<sup>10</sup> as well as in tumor-specific T cells from melanoma patient metastases.<sup>11</sup>

A major limitation of gene microarrays lies in the fact that the resulting data only determine the average gene expression within a given cell population, thus masking the cell-to-cell variations potentially associated with different cellular functions or

outcomes.<sup>12</sup> In order to obtain accurate gene expression patterns among quasi-homogenous cell populations, there arises a need for single-cell analysis providing the highest resolution. In recent years, major efforts have been made to develop precise measurement of single-cell gene expression states in various biological models.<sup>13-16</sup> In particular, Peixoto, Rocha and colleagues<sup>17</sup> described a RT-PCR approach to quantify the expression of 20 different genes simultaneously from a single antigen-specific expanded T cell. Despite studying a relative homogeneous cell population, they demonstrated significant cell-to-cell heterogeneity in terms of gene co-expression. Accumulating data indicate that a seemingly homogeneous population does not represent any one individual cell, but rather reveal unique patterns of gene expression within individual cells.

For an in-depth monitoring of antigen-specific T cell responses, a key endpoint is to relate the expression of specific gene patterns to a distinct cellular phenotype. As such, single-cell gene expression profiling can provide a tight correlation between specific cell surface markers and CD8<sup>pos</sup> T cell functional properties.<sup>18</sup> Specifically it was shown, that each memory- and effector-like CD8<sup>pos</sup> T cell subset displayed a unique pattern of gene expression, with the progressive up-regulation of multiple effector mediators by the same cell along cell differentiation.<sup>18</sup> Cellular immune responses generated following therapeutic vaccines have also been described as highly diverse in terms of phenotype and functionality.<sup>19</sup> Recently Flatz and colleagues identified previously unrecognized subsets of CD8<sup>pos</sup> T cells based upon analysis of gene-expression patterns within single cells and showed that they were differentially induced by different vaccines.<sup>20</sup> These studies emphasize the strong need to delineate the qualitative attributes of vaccine-induced CD8<sup>pos</sup> T cell

responses, not only at the phenotypic/functional levels but as well by defining the genetic signatures of single cells.

In the present study, we investigated the direct *ex vivo* properties of individual virus- and tumor-specific CD8<sup>pos</sup> T cells from healthy donors and from melanoma patients. The latter had been vaccinated with low dose of either the natural or the analog modified Melan-A<sup>MART-1</sup><sub>26-35</sub> peptide, mixed with CpG 7909 and Incomplete Freund's adjuvant (IFA).<sup>21</sup> Previously, we have shown that natural peptide induced T cells, which had enhanced overall functionality and increased capacity to recognize tumor cells compared to T cells stimulated by the analog peptide.<sup>21</sup> Recently, we applied a modified RT-PCR protocol for direct *ex vivo* single T cell analysis,<sup>22,23</sup> and found that non-dominant CD8<sup>pos</sup> T cell clonotypes showed similar activation and differentiation as their dominant counterparts following natural peptide vaccination.<sup>24</sup> Here we extended the highly sensitive and specific single-cell approach to the analysis of multiple memory/homing- (*CD27*, *IL7R*, *EOMES*, *CXCR3*, and *CCR5*) and effector- (*IFNG*, *KLRD1*, *PRF1*, and *GZMB*) associated genes, which allowed us to detect qualitative differences within individual T cells after vaccination with natural versus analog peptide. Our data revealed a vast co-expression of memory/homing- and effector-related genes in T cells induced by vaccination with natural peptide, similar to protective CMV-specific T cells, thus suggesting a higher degree of functional diversity which may be important for mounting efficient responses to pathogens or tumors.

## **MATERIALS AND METHODS**

### *Ethics statement*

The clinical studies were designed and conducted according to the relevant regulatory standards, and approved by (i) the ethical commission of the University of Lausanne (Lausanne, Switzerland), (ii) the Protocol Review Committee of the Ludwig Institute for Cancer Research (New York, USA), and (iii) Swissmedic (Bern, Switzerland). Patient recruitment, study procedures and blood withdrawal from patients and healthy donors were done upon written informed consent.

### *Patients and vaccination protocol*

Four HLA-A\*0201-positive patients with stage III/IV metastatic melanoma were included in a phase I clinical trial (LUD-00-018; [www.clinicaltrials.gov](http://www.clinicaltrials.gov), NCT00112229) of the Ludwig Institute for Cancer Research and the Multidisciplinary Oncology Center.<sup>21,25</sup> Patients received monthly low-dose vaccinations injected subcutaneously with 100 µg of either the Melan-A<sup>MART-1</sup><sub>26-35</sub> unmodified natural peptide (EAAGIGILTV) or the Melan-A<sup>MART-1</sup><sub>26-35</sub> analog A27L peptide (ELAGIGILTV), mixed with 0.5 mg CPG 7909 / PF-3512676 (provided by Pfizer/Coley Pharmaceutical Group; USA) and emulsified in Incomplete Freund's Adjuvant (IFA) (Montanide ISA-51; Seppic, Puteaux, France).<sup>21</sup>

### *Cell preparation, antibodies, and flow cytometry*

Peripheral blood mononuclear cells (PBMCs) were cryopreserved in RPMI 1640, 40% FCS and 10% DMSO following a Ficoll-Paque gradient centrifugation.

Phycoerythrin (PE)-labeled HLA-A\*0201/peptide multimers with A27L Melan-A<sup>MART-1</sup><sub>26-35</sub> (ELAGIGILTV), EBV BMLF1<sub>280-288</sub> (GLCTLVAML), and CMV pp65<sub>495-503</sub> (NLVPMVATV) were synthesized as described previously.<sup>26</sup> CD8<sup>pos</sup> T cells were positively enriched using a MiniMACS device (Miltenyi Biotech, Bergish Gladbach, Germany), resulting in > 90% CD3<sup>pos</sup>CD8<sup>pos</sup> cells. Bulk CD8-enriched T cells were stained using the following 5-color stain combination: (a) FITC-conjugated anti-CD8 (BD Biosciences, Allschwil, Switzerland), (b) PE-conjugated anti-CD3 (BD Biosciences), (c) PE-Texas Red-conjugated anti-CD45RA (Beckman Coulter, Nyon, Switzerland), (d) APC-conjugated anti-CD28 (BD Biosciences), and (e) PE-Cy7-conjugated anti-CCR7 (BD Biosciences). Antigen-specific CD8-enriched T cells were first stained in PBS, 0.2% BSA, 50 µM EDTA with PE-HLA-A2/peptide multimers (1 µg/ml, 60 min, 4°C) followed by 20 min at 4°C with (a) FITC-conjugated anti-CD28 (BD Biosciences), (b) PE-Texas Red-conjugated anti-CD45RA (Beckman Coulter), (c) APC-Cy7-conjugated anti-CD8 (BD Biosciences), and (d) anti-CCR7 purified mAb (BD Biosciences) followed by APC-conjugated goat anti-rat IgG Ab (Caltag Laboratories, Burlingame, UK). Defined T cell subpopulations were then sorted as five-, two- or single-cells on a FACSVantage or a FACS Aria (BD Biosciences), and data were analyzed using FlowJo<sup>TM</sup> (TreeStar, Ashland, USA) software. For *in vitro* T cell cloning, 600 cells from defined subpopulations were sorted into tubes, and further processed as described thereafter. Manipulations were done at 4°C, avoiding gene expression alteration due to staining and sorting procedures. Immediate reanalysis of the FACS-sorted subpopulations revealed over 98% of purity.

Direct ex vivo in-well cell lysis, and reverse transcription (RT)

Prior to FACS sorting, 10 ml of “Lysis buffer” was prepared using 9.22 ml RNase free water molecular biology grade (AppliChem, Darmstadt, Germany), 400  $\mu$ l of 0.1 M DTT (AppliChem), 80  $\mu$ l of 10 mg/ml tRNA (Roche Pharma, Reinach, Switzerland), 300  $\mu$ l of 100% Triton X-100 (Sigma-Aldrich, Buchs, Switzerland) and stored in 1 ml aliquots at -20°C till further use. The “5X RT buffer” was prepared using 12.5 ml 1 M Tris-HCl (pH 8.3; AppliChem), 6.25 ml of 3 M KCl (AppliChem), 750  $\mu$ l of 1 M MgCl<sub>2</sub> (AppliChem) in 30.5 ml RNase free water for a final volume of 50 ml.

For direct *ex vivo* lysis of FACS-sorted five-, two- or single-cells, 96-well V-bottom plates were prepared by adding 15  $\mu$ l/well of a freshly prepared lysis/RT mix containing 6.3  $\mu$ l of “Lysis buffer”, 3  $\mu$ l of “5X RT buffer”, 1.5  $\mu$ l of 0.1 M DTT, 0.75  $\mu$ l of 10 mM dNTPs (Invitrogen/ Life Technologies Corporation, Zug, Switzerland), 0.25  $\mu$ l of 100 ng/ $\mu$ l oligo-(dT) (Metabion, Martinsried, Germany), 0.4  $\mu$ l of MMLV-RT enzyme (Invitrogen), 0.2  $\mu$ l of RNasin (Promega, Madison, WI), and 2.6  $\mu$ l RNase free water. Cells from (i) bulk CD3<sup>pos</sup>CD8<sup>pos</sup> naive (CCR7<sup>pos</sup>CD45RA<sup>pos</sup>CD28<sup>pos</sup>) and EMRA (CCR7<sup>neg</sup>CD45RA<sup>pos</sup>CD28<sup>neg</sup>) T cells, (ii) CD8<sup>pos</sup> tumor-specific effector-memory EM28<sup>pos</sup> (CCR7<sup>neg</sup>CD45RA<sup>neg</sup>CD28<sup>pos</sup>) and EM28<sup>neg</sup> (CCR7<sup>neg</sup>CD45RA<sup>neg</sup>CD28<sup>neg</sup>) T cells, and (iii) CD8<sup>pos</sup> virus-specific EM28<sup>pos</sup> (CCR7<sup>neg</sup>CD45RA<sup>neg</sup>CD28<sup>pos</sup>) and EMRA (CCR7<sup>neg</sup>CD45RA<sup>pos</sup>CD28<sup>neg</sup>) T cells were directly sorted in 96-well V-bottom plates containing 15  $\mu$ l of lysis/RT mix.

Following *ex vivo* flow cytometry sorting, the plates were covered with a plastic adhesive cover and incubated at 37°C for 1 hour followed by a quick chill on ice. This allowed a direct *ex vivo* in-well cell lysis and reverse transcription to cDNA. The

plates were centrifuged at 1500 rpm for 1 min and transferred overnight to -80°C. The next day, the plates were thawed, and the content of each well was transferred to 0.5 ml Eppendorf tubes. The tubes were placed at 90°C for 3 min to heat-inactivate the MMLV-RT enzyme, chilled on ice for 5 min and stored at -80°C until further use.

### *Global cDNA amplification*

This procedure required a purification step (cDNA precipitation) followed by the addition of a homopolymer (dA) sequence to the 3'-OH end of the cDNA. Global cDNA amplification was then carried out using a single modified 61-mer oligo-(dT) primer as adapted from Brady and Iscove<sup>27</sup> and Sauvageau et al.<sup>28</sup>

cDNA precipitation: cDNA (from each tube stored at -80°C) was precipitated overnight at -80°C by adding 7.5 µl of 7.5 M NH<sub>4</sub>-acetate (AppliChem), 3 µl of 10 mg/ml glycogen (Roche), and 45 µl of 100% ethanol. The tubes were then centrifuged at 4°C for 20 min (13000 rpm), and the supernatant was discarded carefully. cDNA pellets were washed with 150 µl of ice cold 70% ethanol and centrifuged at 4°C for 15 min (13000 rpm). After removing the supernatant, the pellets were air-dried for 45 to 60 min at room temperature.

Homopolymeric 3'-oligo-(dA) tailing: The dried pellets were resuspended in 5 µl of tailing mix containing 0.25 µl of 10 mM dATP (Axonlab, Le Mont-sur-Lausanne, Switzerland), 0.08 µl of terminal deoxynucleotidyl transferase (TdT 30 U/ul; Promega), 1 µl of 5X tailing buffer (distributed with the TdT enzyme by the manufacturer), and 3.7 µl RNase free water. The tubes were then incubated at 37°C in a water bath for 30 min followed by heat inactivation at 90°C for 3 min. After a quick chill on ice, tubes were centrifuged briefly at 13000 rpm.

Global cDNA amplification (cDNA<sup>plus</sup>): “5X PCR buffer” with a final 2 mM MgCl<sub>2</sub> concentration contained 250 mM of KCl (AppliChem), 50 mM of Tris-HCl (pH 8.8; AppliChem), 0.5 mg/ml BSA (bovine serum albumine; Roche) and 10 mM MgCl<sub>2</sub>. Aliquots of the “5x PCR buffer” were prepared and stored at -20°C. The PCR mix-A was prepared on ice and contained 8 µl of 5X PCR buffer, 1 µl of oligo-(dT) Iscove 61-mer primer (HPLC purified, 1 µg/µl, 5'-CAT GTC GTC CAG GCC GCT CTG GGA CAA AAT ATG AAT TCT TTT TTT TTT TTT TTT TTT T-3'; Metabion), 1 µl of 10 mM dNTP (Sigma), 2.5 µl of 10% Triton-X100 (Sigma) and 22.5 µl RNase free water. Into each tube containing the 3' oligo-(dA)-tailed cDNA, 35 µl of PCR mix-A was added followed by two drops of mineral oil (Eurobio, Les Ulis, France). Tubes were placed into a PCR machine (BioLabo, Maizy, France) and the cDNA was denatured by heating at 90°C for 3 min followed by an immediate addition of 10 µl of PCR mix-B containing 2 µl of 5X PCR buffer, 1 µl Taq polymerase (5 U/ul; Sigma) and 7 µl RNase free water prior starting the PCR reaction. The PCR was carried out for first 5 cycles (50 s at 94°C; 2 min at 37°C; 9 min at 72°C) followed by 35 cycles (50 s at 94°C; 90 s at 60°C; 8 min at 72°C) and a final extension for 8 min at 72°C. This cDNA<sup>plus</sup> was stably stored at -80°C for several months or years. All *ex vivo* five-, two-, and single-cell cDNA samples were processed with the same rigorous approach to allow direct comparison among individuals and subsets.

### *Gene-specific PCR*

To avoid PCR contamination, the PCR mixes were prepared in a clean and different laboratory area than the ones used for single-cell cDNA preparation and global

amplification (cDNA<sup>plus</sup>). Gene signature of each individual cell was identified by gene-specific PCRs using 1 µl of amplified cDNA<sup>plus</sup> in 20 µl volumes of 4 µl of “5X PCR buffer” with a final 1.5 mM MgCl<sub>2</sub> concentration, 0.4 µl of 10 mM dNTPs, 0.4 µl each forward and reverse specific primers designed to amplify mRNA sequences of interest (100 ng/µl; Metabion), 0.1 µl of Taq polymerase *JumpStart* (5 U/µl, Sigma), and 13.7 µl of RNase free water. The PCR amplification was carried out at 94°C for 3 min followed by 38-40 cycles (30 s at 94°C; 45 s at 58°C or 60°C; 1 min at 72°C) followed by 1 cycle (10 min at 72°C). The PCR products were visualized after electrophoresis on a 1.5% agarose gel. Typically, we used H<sub>2</sub>O for the negative PCR control, while 1 x 10<sup>3</sup> PBMCs from a healthy individual were used as positive PCR control.

For specific gene expression analysis, we carefully designed our specific primers in such a way that they are usually located within the first 1000 bp upstream of the 3'-poly(dA) end of the mRNA sequence, and whenever possible inter-exonic, thus excluding genomic DNA amplification. We used the following primers: *GAPDH*: 5'-GGACCTGACCTGCCGTCTAG-3'; rev-5'-CCACCACCCTGTTGCTGTAG-3', *β2 microglobulin*: 5'-CCAGCAGAGAATGGAAAGTC-3'; rev-5'-GATGCTGCTTACATGTCTCG-3', *CCR7*: 5'-CCAGGCCTTATCTCCAAGACC-3'; rev-5'-GCATGTCATCCCCACTCTG-3', *CD27*: 5'-ACGTGACAGAGTGCC TTTTCG-3'; rev-5'-TTTGCCCGTCTTGTAGCATG-3', *IL7R* (IL-7Rα/CD127): 5'-ATCTTGGCCTGTGTGTTATGG-3'; rev-5'-ATTCTTCTAGTTGCTGAGGAAACG-3'; *EOMES* (eomesodermin): 5'-AGCAGGCTGTGAACATTGG-3'; rev-5'-TTGACTCCTGGGCCTAGTATC-3', *CXCR3*: 5'-GCACCATTGCTGCTCCTTAG-3'; rev-5'-TACGCCATGCCTTGTACTCC-3', *CCR5*: 5-TCAGCAGGAAGCAA CGAAGG-3'; rev-5'-TCTTTGACTTGGCCCAGAGG-3', *KLRD1* (CD94) (located

at -2611 bp): 5'-GTGGGAGAATGGCTCTGCAC-3'; rev-5'-TGAGCTGTTGCTTA  
 CAGATATAACGA-3', *IFNG* (IFN- $\gamma$ ): 5'-GCCAACCTAAGCAAGATCCCA-3';  
 rev-5'-GGAAGCACCAGGCATGAAATC-3', *PRF1* (Perforin): 5'-TTCACTGCC  
 ACGGATGCCTAT-3'; rev-5'-GCGGAATTTTAGGTGGCCA-3', *GZMB*  
 (Granzyme B): 5'-GCAGGAAGATCGAAAGTGCGA-3'; rev-5'-GCATGCCAT  
 TGTTTCGTCCAT-3'.

#### *Generation of T cell clones*

HLA-A2/multimer<sup>pos</sup> CD8<sup>pos</sup> T cell subsets (EM28<sup>pos</sup>, EM28<sup>neg</sup>, and EMRA) were sorted by flow cytometry,<sup>29,30</sup> cloned by limiting dilution, and expanded in RPMI 1640 medium supplemented with 8% human serum, 150 U/ml recombinant human IL-2 (rhIL-2; a gift from GlaxoSmithKline, Münchenbuchsee, Switzerland), 1  $\mu$ g/ml phytohemagglutinin (PHA; Sodiag, Losone, Switzerland) and 1  $\times$  10<sup>6</sup>/ml irradiated allogeneic PBMC (3000 rad) as feeder cells. T cell clones were expanded by periodic (every 15 days) restimulation with PHA, irradiated feeder cells, and rhIL-2. Cells (1  $\times$  10<sup>4</sup>) from T cell clones, were directly processed through direct cell lysis and cDNA synthesis as described above without undergoing the global cDNA amplification procedure.

#### *TCR V $\beta$ chain repertoire and clonotype analysis*

TCR BV repertoire analysis or CDR3 spectratyping was performed as described previously.<sup>29,30</sup> Briefly, pools of the equivalent of 50 cells were subjected to individual PCR in non-saturating conditions using a set of previously validated fluorescent-labeled forward primers specific for the 22 TCR BV subfamilies and one

unlabeled reverse primer specific for the constant region of the  $\beta$  chain of the TCR.<sup>31</sup> This analysis represented a screening step. Once positive TCR BV subfamilies were identified, the following step consisted in subjecting each individually generated single-cell cDNA sample, and in parallel *in vitro* generated T cell clone to TCR BV PCRs. Separation and detection of amplified fragments containing the entire CDR3 segment was performed in the presence of fluorescent size markers on an ABI PRISM 310 Genetic Analyzer (AppliedBiosystems/Life Technologies Corporation, Zug, Switzerland) and data were analyzed with GeneScan 3.7.1 (AppliedBiosystems). In the last step, PCR products of interest were directly purified and sequenced with the reverse primer (Fasteris SA, Geneva, Switzerland). Clonotypic primers for several CDR3 sequences were validated and used in clonotypic PCR for determination of clonotype frequencies as previously reported.<sup>29,30</sup> All direct *ex vivo* single-cell and *in vitro* T cell clone cDNA samples were processed with the same rigorous approach to allow direct comparison among individuals and subsets.

#### *Enzyme Linked Immunospot (Elispot) assay*

To evaluate the *ex vivo* functional potential of tumor-specific T cells from vaccinated melanoma patients, IFN- $\gamma$  Elispot assays were performed as described.<sup>25</sup> Briefly, plates were coated overnight with human IFN- $\gamma$ -specific antibodies (Diaclone, Biotest, Rapperswil, Switzerland), and washed. In 3-6 replicates,  $1.66 \times 10^5$  PBMCs/well were stimulated with 10  $\mu\text{g/ml}$  of the native Melan-A<sup>MART-1</sup><sub>26-35</sub> peptide (EAAGIGILTV) for 16 hours at 37°C. Cells were removed, and plates developed with a second biotinylated antibody to human IFN- $\gamma$  and streptavidin-alkaline phosphatase (Diaclone, Biotest). The spots were revealed with BCIP/NBT substrate and counted with an automatic reader (Bioreader 2000; BioSys GmbH, Karben,

Germany). The proportion of primed tumor-specific CD8<sup>pos</sup> T cells following multimer, CD8, CD45RA and CCR7 co-stainings was determined by flow cytometry on the same batch of cryopreserved cells. Elispot-forming T cells are expressed as percentage of non-naive (non-CD45RA<sup>pos</sup>CCR7<sup>pos</sup>) multimer<sup>pos</sup> CD8<sup>pos</sup> T cells.

#### *Chromium release and target cell killing assays*

Tumor-specific T cell clones were generated *in vitro* from four patients with melanoma following analog/ELA (n = 2) or natural/EAA (n = 2) peptide vaccination. Lytic activity and antigen recognition was assessed functionally in 4-hour <sup>51</sup>Cr-release assays using T2 target cells (HLA-A\*0201<sup>pos</sup>/TAP<sup>neg/neg</sup>) pulsed with serial dilutions of the native Melan-A<sup>MART-1</sup><sub>26-35</sub> peptide (EAAGIGILTV). The percentage of specific lysis was calculated as  $100 \times (\text{experimental} - \text{spontaneous release}) / (\text{total} - \text{spontaneous release})$ .

#### Statistical analyses

For quantitative comparison, linear regression analysis with 95% confidence intervals or two-tailed unpaired *t* test were performed with Prism 5.0 (La Jolla, California, USA), while one-way ANOVA test was performed by SPSS statistical version 19 (IBM, Chicago, USA). Co-expression pie charts were compared with each other using 10'000 permutations calculated with the Software SPICE 5.2 (NIH, Bethesda, USA).

## RESULTS

### *Global cDNA amplification and validation of single-cell gene expression analysis*

Following FACS-sorting of CD8<sup>pos</sup> T cell subsets of interest (bulk or antigen-specific cells), single cells were directly lysed in-well before reverse transcription of mRNA to cDNA, and subsequent global amplification of total cDNA (Fig. 1). The basic principle of this approach required that the target cellular cDNA be flanked by known sequences to which the amplification primers can anneal and initiate polymerization. As such, the reverse transcription was completed using an oligo-(dT) primer that annealed to the poly(A) tail present at the 3' end of most mRNA molecules (Fig. 1A; step 2). Next, a homopolymer (dA) sequence was added to the 3'-OH end of the cDNA using terminal deoxynucleotidyl transferase (Fig. 1A; step 3). Global PCR amplification of the (dA)/(dT) flanked cDNAs was then carried out using a single 61-mer modified oligo-(dT) primer, as previously described by Brady and Iscove.<sup>27</sup> Specifically, priming of the cDNA during global PCR amplification was initiated via annealing of the (dT) region of this modified oligo-(dT) primer to the poly(dA) regions present at the 3' termini of the cDNA molecules (Fig. 1A; step 4). Since our approach uses oligo-(dT) based mRNA amplification, the only pre-requisite for the present technique is the careful design of primers such that they fall within the 1000 bp from the 3' end of mRNA. The efficiency of globally amplified cDNA from single CD8<sup>pos</sup> T cells, also termed cDNA<sup>plus</sup> (Fig. 1A; step 5), was then analyzed for the expression of housekeeping genes like glyceraldehyde 3-phosphate dehydrogenase (*GAPDH*) and beta-2-microglobulin (*B2M*) by semi-quantitative PCR. This represents a pre-screening step allowing selecting for positive *GAPDH* and/or *B2M* single-cell samples which will be further subjected to specific gene expression PCRs. The average efficiency of > 2400 single cells analyzed was close to 80% and 90%

using *GAPDH* and *B2M*, respectively (Fig. 1B), demonstrating robust reproducibility of our cDNA<sup>plus</sup> approach.

*Sensitivity and specificity of the single-cell cDNA<sup>plus</sup> approach*

Serial dilutions of single-cell cDNA<sup>plus</sup> from sorted bulk CD8<sup>pos</sup> T cells and from sorted naive and EMRA/effector CD8<sup>pos</sup> T cell subsets were compared to cDNA<sup>plus</sup> from five- and two-cell samples (Fig. 2A). Amplified poly-(dA) cDNA<sup>plus</sup> allowed the detection of robust PCR signals for *GAPDH* in bulk CD8<sup>pos</sup> T cells, as well as for the homing chemokine receptor *CCR7* (*CCR7*) in naive cells and for granzyme B (*GZMB*) in EMRA cells, even at high dilutions ( $10^{-4}$ ). Our results show that the PCR sensitivity with cDNA<sup>plus</sup> obtained from single cells was comparable to PCR with cDNA<sup>plus</sup> isolated from five-cells and two-cells samples.

We next determined the specificity of the single-cell approach by assessing the expression of a panel of genes known to be differentially expressed in the naive CD8<sup>pos</sup> T cell subset compared to the EMRA/effector differentiated subset (Fig. 2B). As expected, most of the naive T cell cDNA<sup>plus</sup> samples yielded detectable expression of *CCR7*, *CD27* (a member of the TNF-receptor superfamily) and *IL7R* (the cytokine receptor IL-7R $\alpha$ ). In sharp contrast, these mRNA transcripts were rarely found in the EMRA/effector T cells, which instead contained significant levels of mRNA coding for effector mediators such as the natural killer cell-receptor CD94 (*KLRD1*), IFN- $\gamma$  (*IFNG*), perforin (*PRF1*) or granzyme B (*GZMB*). Taken together, these data demonstrate the remarkable sensitivity and specificity of the single-cell cDNA<sup>plus</sup> approach, wherein CD8<sup>pos</sup> T cells can be individually sorted directly *ex vivo*

according to well-defined subpopulations and specific-gene expression profiles subsequently analyzed (Fig. 2).

*TCR  $\beta$ -chain repertoires and clonotype frequencies determined by the direct ex vivo single-cell approach strongly correlate with results obtained by in vitro T cell cloning*

Our single-cell gene expression analysis approach allows analyzing individual TCR-BV-CDR3 $\beta$  sequence motifs. Therefore, we determined the TCR clonotype repertoires of tumor- and virus-specific CD8<sup>pos</sup> T cell subpopulations. Specifically, individual cells from tumor-specific CD8<sup>pos</sup> T lymphocytes from melanoma patients following vaccination with either natural/EAA or analog/ELA Melan-A<sup>MART-1</sup><sub>26-35</sub> peptide were FACS-sorted and characterized for their TCR clonotype repertoire. The same experimental procedure was performed on EBV- (Epstein-Barr-virus) and CMV- (Cytomegalovirus) specific single T cells from healthy donors.

The TCR clonotype repertoire analysis of directly ex vivo sorted single tumor- and virus-specific T cells was first compared with that of single T cells generated by *in vitro* limiting dilution cultures, which has long been the method of choice for assessing TCR BV gene segment usage.<sup>19</sup> Despite a large usage of the 22 different TCR BV families, in line with our previous reports,<sup>29,30</sup> we observed highly similar proportions of TCR BV family usage (Fig. 3A) and of individual TCR clonotype signatures (Fig. 3B) with both the direct *ex vivo* single-cell and the *in vitro* T cell cloning approaches. In particular, the single-cell analysis confirmed that TCR  $\beta$ -chain repertoires were broader after vaccination with natural than analog peptide.<sup>29</sup> Moreover, the EBV-specific TCR repertoire showed a preferential usage of TCR

BV2 and BV4 gene segments with a wider variety of T cell clonotypes as compared to the restricted CMV-specific TCR  $\beta$ -chain repertoire.<sup>30</sup> Remarkably, the relative proportions of dominant T cell clonotypes, and to a lesser extent of sub-dominant clonotypes (with frequencies < 20%), were found to be very similar using either of the two techniques, resulting in a high correlation coefficient (Fig. 3C). Collectively, our results based from the direct *ex vivo* single-cell cDNA<sup>plus</sup>-based analysis are in excellent agreement with those obtained with large numbers of *in vitro* generated T cell clones.

*Natural peptide vaccination induced tumor-specific CD8<sup>pos</sup> T cells with superior effector functions compared to vaccination with the analog peptide*

Vaccine-induced Melan-A<sup>MART-1</sup>-specific CD8<sup>pos</sup> T lymphocytes have been shown to exhibit an “effector-memory” (EM; CD45RA<sup>neg</sup>CCR7<sup>neg</sup>) phenotype<sup>32</sup> and to include two distinct functional subsets distinguished by CD28 expression<sup>24,33</sup>; (i) CD28<sup>pos</sup> (defined thereafter as EM28<sup>pos</sup> or early-differentiated) T cells and (ii) CD28<sup>neg</sup> (EM28<sup>neg</sup> or late-differentiated) cells (Fig. 4A). In contrast, EBV- and CMV-specific CD8<sup>pos</sup> T cells are mostly composed of early- (EM28<sup>pos</sup>) and late-differentiated (EMRA; CD45RA<sup>pos</sup>CCR7<sup>neg</sup>CD28<sup>neg</sup>) subsets, but they vary in the proportions of these subsets.<sup>30</sup> EM28<sup>neg</sup> and EMRA subsets can be both defined as late-differentiated “effector-like” T lymphocytes.<sup>34</sup> Accumulation of CD28<sup>neg</sup> tumor-specific T cell subsets occurred following vaccination with the natural/EAA Melan-A<sup>MART-1</sup><sub>26-35</sub> peptide, comparable to that of protective T cell responses specific for CMV (Fig. 4A). The proportion of “early-differentiated” CD28<sup>pos</sup> T cells was maintained after peptide vaccination and was very similar between tumor- and virus-specific T cell responses.

In line with our previous reports,<sup>21,24</sup> vaccination with the natural/EAA peptide induced more robust T cell activation with increased proportions of IFN- $\gamma$  producing T cells by Elispot assays as compared to the T cell responses following vaccination with the analog/ELA Melan-A<sup>MART-1</sup><sub>26-35</sub> peptide (Fig. 4B). Moreover, natural/EAA peptide vaccine-induced T cell clones derived from EM28<sup>pos</sup> cells exhibited superior target cell killing responses, compared to T cell clones from the corresponding subset upon analog/ELA peptide vaccination (Fig. 4C). In contrast, most of tumor-specific T cell clones derived from the differentiated “effector-like” EM28<sup>neg</sup> subset showed similar efficient lysis capacity, irrespectively of the peptide used for vaccination.

*Extended co-expression of memory/homing- and effector-associated mRNA transcripts in single tumor-specific T cells induced by natural peptide vaccination*

The powerful single-cell based approach enabled the assessment of expression of memory- and effector-related gene patterns from individual tumor- and virus-specific CD8<sup>pos</sup> T cells directly *ex vivo*. We designed PCR primers for a panel of genes related to memory and homing (*CD27*, *IL7R*, *EOMES*, *CXCR3* and *CCR5*) or effector (*IFNG*, *KLRD1*, *PRF1*, and *GZMB*) T cell properties.<sup>20,32,35-40</sup> High expression of memory/homing-associated mRNA transcripts was observed in the early-differentiated EM28<sup>pos</sup> tumor- and virus-specific subsets, while expression of effector-associated gene mediators was preferentially found in the late-differentiated EM28<sup>neg</sup>/EMRA T cells (Fig. 4D and 4E). Interestingly, EM28<sup>pos</sup> EBV-specific T cells had the highest expression of memory/homing-related genes (Fig. 4D), which contrasted to relatively low effector-gene expression (Fig. 4E), in agreement with our previous reports.<sup>24,30</sup> T cell responses induced by the natural/EAA peptide vaccine triggered memory/homing-associated gene expression patterns that were in between

that of persistent EBV and analog/ELA peptide vaccine-induced T cells (Fig. 4D, left panel). Specifically, we observed significantly enhanced expression of *CD27*, *CCR5* and the transcription factor *EOMES* within those T cells, compared to tumor-specific T cells following analog peptide vaccination. Importantly, a large proportion of the natural peptide vaccine-induced T cells expressed as well *IFNG*, *KLRD1* (CD94), *PRF1* and *GZMB* mRNA transcripts (Fig. 4E), even in the less differentiated EM28<sup>pos</sup> T cell compartment where the difference to the analog peptide induced T cells was statistically significant (Fig. 4E, left panel).

Subsequently we analyzed the gene expression polyfunctionality as well as the heterogeneity of co-expression patterns of either memory/homing- or effector-associated genes along cell differentiation (Fig. 5). We found that vaccination with the analog/ELA peptide induced T cells with only limited co-expression, particularly for effector-associated genes in the early-differentiated EM28<sup>pos</sup> subset (Fig. 5A), and for memory/homing-associated genes in the late-differentiated EM28<sup>neg</sup>/EMRA subsets (Fig. 5B). These data are in sharp contrast to the single T cells induced by vaccination with the natural/EAA peptide, showing impressive gene expression polyfunctionality and co-expression variability of memory/homing- and of effector-associated transcripts (up to 3/4 co-expressing genes). These co-expression patterns were preferentially found in the early-differentiated subset, and resembled those observed in protective CMV-specific T cells (Fig. 5A). These findings indicate a differential process of cell differentiation following natural versus analog peptide vaccination, and show that the peptide used for vaccination determines the functional properties of individual tumor-specific T cells.

*Natural peptide vaccination induced highly diverse individual T cells co-expressing multiple different memory/homing and effector gene patterns directly ex vivo*

To assess the gene expression diversity among vaccine-induced T cells, we analyzed the distributions of tumor- and virus-specific T cells depending on their simultaneous co-expression of both memory/homing- and effector-associated gene transcripts. Single T cells with all possible combinations of gene expression were plotted on three-dimensional matrix (Fig. 6), according to expression of 0 to 5 memory/homing genes (*IL7R*, *CD27*, *EOMES*, *CXCR3*, and *CCR5*) versus 0 to 4 effector-genes (*IFNG*, *KLRD1*, *PRF1* and *GZMB*). The data revealed an extraordinary diversity in terms of memory/homing and effector gene co-expression patterns by individual cells. Specifically, tumor-specific T cells induced by the natural/EAA peptide vaccine frequently co-expressed various combinations of multiple memory/homing- and multiple effector-associated mRNA transcripts (Fig. 6A, right panel). This was best illustrated for the single T cells issued from the early-differentiated EM28<sup>pos</sup> subset, co-expressing up to 5 memory/homing- and 4 effector-related genes.

In contrast, analog/ELA peptide vaccine-induced T cells showed distinct memory/homing and effector-related gene co-expression patterns that were highly dependent on the differentiation stage (Fig. 6A, left panel), in agreement with the above-described results (Fig. 4 and Fig. 5). The early-differentiated EM28<sup>pos</sup> subset primarily expressed memory/homing-associated transcripts, while the late-differentiated EM28<sup>neg</sup> cells mostly expressed effector-associated genes (up to 4 co-expressing transcripts) with only rare memory/homing-gene co-expression (up to 1-2 co-expressing transcripts). Finally, EBV- and CMV-specific T cells displayed memory/effector gene-co-expression patterns that placed them in between those observed for the natural and analog peptide vaccination induced T cells (Fig. 6B).

*Heterogeneity and co-expression of memory/homing and effector gene transcripts by tumor- and virus-specific T cell clonotypes*

We recently reported a progressive restriction in the TCR BV/CDR3 diversity along cell differentiation (from EM28<sup>pos</sup> to EM28<sup>neg</sup>).<sup>24</sup> T cell receptor (TCR) clonotype mapping revealed preferential selection and expansion of co-dominant T cell clonotypes, which made up between 50 to 60% of the differentiated “effector” T cells, but only 25% on average of the early-differentiated EM28<sup>pos</sup> cells, mostly composed of non-dominant clonotypes. A striking observation was that tumor-reactive T cell responses were in several patients dominated by individual clones,<sup>33,41</sup> such as for example BV17.1 clonotype for patient LAU 618 or BV13.1 clonotype for patient LAU 1013 (Fig. 7). This process occurred irrespective of whether natural or analog peptide was used for vaccination, and resembled that observed in EBV and CMV specific T cells.<sup>30</sup>

Here we extended these analyses by assessing the direct *ex vivo* co-expression patterns of memory/homing- and effector-associated genes within the dominant T cell clonotypes that were selected with advanced differentiation, i.e. clonotypes found in both EM28<sup>pos</sup> and EM28<sup>neg</sup> subsets, compared to those that were not (Fig. 7). The memory/homing and effector gene co-expression profiles of all dominant EM28<sup>pos</sup> T cell clonotypes (Fig. 7A) largely overlapped with those of the corresponding early-differentiated EM28<sup>pos</sup> subset (Fig. 5A). For example, BV13.1 clonotype induced by the natural/EAA peptide vaccination (from patient LAU 1013) was highly polyfunctional, with > 3 co-expressing memory/homing and/or effector genes. In contrast, BV17.1, BV3.1 and BV13.2 clonotypes from patient LAU 618 vaccinated with the analog/ELA peptide were globally less polyfunctional (Fig. 7A). In the differentiated EM28<sup>neg</sup> subset, all selected clonotypes showed reduced

memory/homing-related gene co-expression, while maintaining or further acquiring effector-mediated gene co-expression (Fig. 7B).

Importantly, the gene profiles of the EM28<sup>pos</sup> T cell clonotypes that were highly selected with differentiation were more polyfunctional (co-expressing  $\geq 2$  memory/homing- or effector-associated genes) compared to those that were not selected or remained at low frequencies (Fig. 7A). Indeed, many of the unselected (e.g. BV3.1 and BV13.2 clonotypes from LAU 618) or the less frequently selected (e.g. BV7.3/BV14.1/BV13.3 clonotypes from LAU 1013) single T cells exhibited reduced co-expression of mRNAs coding for either memory/homing- or effector-mediating molecules. Of note, dominant T cell clonotypes from EBV-specific T cell responses or from the two other vaccinated melanoma patients could not be included in this study, as we were unable to identify sufficient numbers of co-existing single T cell clonotypes shared between both EM28<sup>pos</sup> and EM28<sup>neg</sup>/EMRA subsets.

Collectively, our data show that the single-cell approach represents a powerful tool to characterize fine differences within the TCR-based clonotype selection and composition of tumor-reactive CD8<sup>pos</sup> T cells along T cell differentiation (early-versus late-differentiation). It further suggests that the selection of T cell clonotypes with cell differentiation may not strictly depend on TCR-related parameters (e.g. TCR-pMHC affinity/avidity), but may as well involve the co-expression within the same cell of particular memory/homing- and effector-mediated gene patterns.

## DISCUSSION

The results presented in this study offer novel insights on cellular heterogeneity and polyfunctionality within tumor- and virus-specific CD8<sup>pos</sup> T cell sub-populations. It is becoming increasingly clear that analyses based on cell averages within a given population may be misleading. Even within carefully sorted cellular populations, there remains significant cellular diversity. It is possible to discriminate immune cell heterogeneity at three different levels. First, T cells may be identified at the sub-population level of relatively diverse memory- and effector-related T cells based on their expression of costimulatory molecules CD27 and CD28 and other surface markers.<sup>36</sup> At a second level, it is also possible to demonstrate immune cell heterogeneity based on the polyfunctionality of T cell sub-populations. Finally, a third level of immune cell heterogeneity is now perceptible at the basic biological unit: the individual cell. The notion of varying degrees of polyfunctionality of individual cells reveals the diversity of seemingly well-defined sub-populations or subsets, demonstrating the heterogeneity of antigen-specific T cell responding to antigenic challenges.

The fast advancing field of multiparameter flow cytometry combined with novel strategies for gene expression profiling of antigen-specific T cells of particular phenotypes have opened new opportunities for performing detailed analyses at the individual cell level. For this purpose, we previously developed a strategy consisting of cell lysis and cDNA synthesis in a single-step procedure, followed by a modified PCR protocol that relies on the detection of specific cDNAs after global amplification of expressed mRNAs<sup>22,23</sup> (Fig. 1). This method yielded sufficient cDNA from as few as five cells, which allowed us to follow tumor-specific T cells before and after therapeutic peptide vaccination,<sup>33,41</sup> as well as EBV- and CMV-specific T cells from

healthy individuals over time.<sup>30</sup> Recently, we have optimized the above-described strategy of global cDNA amplification at the single-cell level for direct *ex vivo* monitoring of gene expression profiles<sup>24</sup> (Fig. 2 and Fig. 4). Other methods have been documented to quantify the gene expression profile of a single-cell, all with their own uses, advantages and drawbacks.<sup>42-46</sup> Without contesting the validity and specificity of these techniques, we believe that our approach has the added advantages of practicality, low-cost and adaptability. By utilizing standard biological techniques (reverse transcription and semi-quantitative PCR), this single-cell method is affordable, as it does not require the engineering of novel microfluidic platforms<sup>14</sup> or the assistance of robotic technologies, except for an efficient sorting facility. Nonetheless the implementation of automated steps is warranted to minimize sample manipulation, which may lead to contamination and loss of material.

Furthermore, our method does not require pre-customization of genes for selective amplification and therefore is completely flexible regarding the genes analyzed. Each PCR needs only small volumes (0.5 to 1  $\mu$ l) of the total cDNA<sup>plus</sup> sample, the remainder can thus safely be stored at -80°C for any future analysis. By combining single-cell isolation with the characterization of defined TCR BV-CDR3 sequences, the TCR repertoire diversity and clonal composition of well-defined antigen-specific T cell subpopulations can also be characterized, and are in excellent agreement with the data obtained with large numbers of *in vitro* generated T cell clones (Fig. 3). In the present study, we examined the expression of cell surface markers/receptors and cytoplasmic proteins known to be associated with either effector or memory/homing functions. *IFNG*, *KLRD1*, *GZMB* and *PRF1* all encode for proteins well characterized to be expressed by effector CD8<sup>pos</sup> T cells.<sup>32,40</sup> Conversely, *CD27*<sup>38</sup> and *IL7R*<sup>37</sup> are used as markers of the memory phenotype. *CCR5* and *CXCR3* are involved in

cellular migration and homing into inflamed tissue and are upregulated on memory cells.<sup>20,35,47,48</sup> Finally, although *EOMES* can drive the differentiation of effector CD8<sup>pos</sup> T cells in partnership with T-bet,<sup>39</sup> it is also involved in central-memory T cell differentiation and longevity.<sup>49</sup> Future direction involves the fine characterization at the single-cell level of transcriptional factors and their co-expression patterns involved in the regulation and differentiation of early- and late-differentiated antigen-specific CD8<sup>pos</sup> T cells.

Single-cell analyses have been documented in various fields of research, but few studies have focused on the heterogeneity of T cell responses. Recent data suggest that the T cell heterogeneity begins at the level of cell division. By monitoring the cellular localization of key immune cell fate mediators, Chang et al. demonstrated that, following initial antigen encounter, naive T cells undergo stem cell-like asymmetrical cell division yielding daughter cells with either memory or effector properties.<sup>50</sup> In a different *in vivo* model, the microinjection of a single naive T cell was also shown to repopulate a host with a progeny of differentiated effector and memory cells.<sup>51</sup> These studies speak of the diversification potential of naive T cells, but yet do not address the polyfunctionality of individual cells. Single-cell based gene expression approaches were particularly successful in gaining insights in T cell heterogeneity and intrinsic polyfunctionality following primary antigenic stimulation or therapeutic vaccination.<sup>20,52</sup> Our data are in line with these observations and further illustrate the increased level of diversity in terms of simultaneous co-expression of memory/homing- and effector-related genes, which we observed for both tumor- and virus-specific T cells, within defined subsets (EM28<sup>pos</sup> and EM28<sup>neg</sup>/EMRA) and specific TCR clonotypes (Fig. 5, Fig. 6 and Fig. 7).

Polyfunctional antigen-specific CD8<sup>pos</sup> T cells have been commonly observed in response to viral diseases, both for acute (e.g. influenza) as well as for persistent but efficiently controlled (e.g. CMV and EBV) infections. Similarly, a higher degree of polyfunctionality was also described within a small group of HIV-infected individuals named long-term non-progressors compared to those with progressing HIV disease.<sup>53,54</sup> It seems likely that protective T cell responses against viral infections or malignant diseases rely on both phenotypic and functional heterogeneity with a greater than ever polyfunctionality. Along these lines, Newell and coworkers<sup>55</sup> have very recently described a large degree of functional diversity even among CD8<sup>pos</sup> T cells with the same specificity, thus allowing a remarkable degree of flexibility in responding to pathogens. Such extreme functional diversity may thus represent the successful step for tumor eradication and/or long-term survival in chronic diseases.<sup>56</sup>

Peptide-based cancer vaccines have often been performed with analog peptide antigens designed for enhanced MHC class I binding. It is important to elucidate how these modifications may affect the generation of vaccine-specific T cell clonotype repertoires and tumor recognition efficiency by those T cells. We previously reported that compared with vaccination with the analog/ELA Melan-A<sup>MART-1</sup><sub>26-35</sub> peptide,<sup>57</sup> natural/EAA peptide vaccination generates T cells with enhanced activation and effector functions.<sup>21</sup> These observed differences could not be explained by structurally distinct TCRs, since vaccination with natural and analog peptide induced TCR repertoires with structurally conserved features of TCR $\alpha\beta$  chains.<sup>29</sup> However, when Cole and colleagues<sup>58</sup> evaluated the intra-individual clonotypic responses to both natural and analog peptide, based on samples derived from the same naive T cell pool, they could show that the analog peptide primed T cells with largely different

TCRs compared with those primed with the natural antigen. More recently, we demonstrated that the observed superior tumor activity of the natural peptide induced T cells resulted from effector functions developing properly in nearly all dominant and low/non dominant tumor-specific T cell clonotypes, in contrast to T cells generated following natural Melan-A<sup>MART-1</sup><sub>26-35</sub> peptide vaccination.<sup>24</sup> Here, we strengthen these findings by uncovering a previously unknown level of gene expression diversity among natural peptide induced T cells, with the simultaneous co-expression of memory/homing- and effector-related genes by the same cell. Our results further suggest that the natural peptide promotes a broader diversification of tumor-specific T cells, which may favor their activation and effector potential. Strikingly, memory/effector gene co-expression reflected a polyfunctionality that was also observed at the clonotypic level (Fig. 7, data not shown), which may be important for mounting potent immune responses against tumors and pathogens. Overall these data and those by others<sup>58-60</sup> show that a single amino acid substitution within a peptide used for vaccination can have significant consequences on the quality of the T cell response. Further work is needed to elucidate the mechanisms involved in the qualitative superior T cell response induced by natural peptide vaccination. Nevertheless, direct *ex vivo* high-resolution molecular characterization of individual T cells as shown here provides enhanced insights in the processes shaping the functional properties of tumor-specific T cells.

## **ACKNOWLEDGEMENTS**

We thank the patients and blood donors for their dedicated collaboration in this study, and Pfizer and Coley Pharmaceutical Group for providing CpG-ODN PF-3512676/7909. We gratefully acknowledge P. Guillaume, O. Michielin, I. Luescher and P. Romero for essential collaboration and advice. We are also thankful for the excellent help of L. Cagnon, C. Geldhof, N. Montandon, and M. van Overloop.

This study was sponsored and supported by the Swiss National Science Foundation grant 3200B0-118123 and 310030-129670, a grant from the Swiss National Center of Competence in Research (NCCR) Molecular Oncology, and the Ludwig Institute for Cancer Research, NY USA.

**FIGURE LEGENDS**

**Figure 1.** (A) Basic steps involved for global amplification of cDNA from FACS-sorted individual CD8<sup>pos</sup> T cells directly *ex vivo*. (B) Efficiency of single-cell cDNA<sup>plus</sup> as a measure of positive PCR signals for the house-keeping genes *GAPDH* (33 independent experiments including a total of 1709 tested single-cell samples) and/or *B2M* (18 independent experiments including a total of 768 tested single-cell samples). Of note, comparable cDNA<sup>plus</sup> efficiencies were found within the same experiment and among different antigen-specific CD8<sup>pos</sup> T cell subsets (e.g. EM28<sup>pos</sup> versus EM28<sup>neg</sup> versus EMRA), data not shown.

**Figure 2.** Sensitivity and specificity of the single-cell cDNA<sup>plus</sup> approach. (A) Serial dilutions of cDNA<sup>plus</sup> from 5, 2, and 1 cell(s) sorted from bulk CD8<sup>pos</sup>, naive and EMRA CD8<sup>pos</sup> T cell subsets were tested for *GAPDH*, *CCR7* and *GZMB* (Granzyme B) gene expression, respectively. The starting cDNA<sup>plus</sup> (isolated from 5, 2, or 1 cell) was prepared using 10-fold serial dilutions as indicated ( $\text{Log}_{10}$  of the reciprocal of the dilution value). Top panel shows a representative example of gene expression detection along serial dilutions. Bottom panel represents the exact number of positive PCR signals within the tested samples ( $n = 4$ ) for each cDNA<sup>plus</sup> dilution. (B) Gene expression analysis was performed on single-cells sorted from naive ( $n = 29$ ) or EMRA ( $n = 30$ ) CD8<sup>pos</sup> T cell subsets. Data from 10 independent single-cell aliquots are depicted. The cumulative gene expression for all tested naive and EMRA single T cells is shown in the right panel.

**Figure 3.** Comparison of the proportion of TCR V $\beta$ -chain usage (A) and clonotype diversity (B) between the direct *ex vivo* single-cell and the *in vitro* limiting dilution approach. (A) TCR BV family usage was determined on individual tumor-specific CD8<sup>pos</sup> T cells isolated from four patients vaccinated with the natural/EAA or analog/ELA peptide, and from EBV- and CMV-specific CD8<sup>pos</sup> T cells from healthy donors BCL6 and BCL8. Data are depicted as cumulative frequencies of TCR BV family usage of *in vitro* T cell clones versus direct *ex vivo* single T cells. (B) Relative frequencies of T cell clonotypes issued either from the *ex vivo* single-cell or the *in vitro* limiting dilution approach. Each symbol represents the proportion of a given clonotype from late-differentiated EM28<sup>neg</sup> (ELA and EAA) or EMRA (EBV and CMV) T cell subset. ELA, analog peptide vaccination; EAA, natural peptide vaccination. Of note, clonotypes bearing the TCR BV14 gene usage were often under represented by the *ex vivo* single-cell approach. (C) Positive correlation of clonotype frequencies obtained between direct *ex vivo* single-cell cDNA<sup>plus</sup> and *in vitro* single-cell cloning (by linear regression analysis with 95% confidence intervals). The inset shows the correlation between sub-dominant clonotype frequencies ( $\leq 20\%$  of prevalence). (A-C) TCR BV usage and clonotype repertoire analysis was performed as detailed in the Materials and Methods section. *In vitro*: data from single T cell clones generated by *in vitro* limiting dilutions (n = 1505). *Ex vivo*: data from FACS-sorted single T cells and directly processed by cDNA<sup>plus</sup> gene expression amplification (n = 586). The TCR V $\beta$ -chain nomenclature proposed by Arden et al. was used.<sup>61</sup>

**Figure 4.** Functional competence and gene expression analysis of tumor-specific T cells following natural/EAA and analog/ELA peptide vaccination. (A) *Ex vivo*

analysis of circulating tumor-specific T cells in patients vaccinated with the analog (n = 10) or natural (n = 5) peptide, and virus-specific T cells from healthy donors (n = 8). Data are expressed as percentage of CD28<sup>pos</sup> and CD28<sup>neg</sup> cells in multimer<sup>pos</sup> CD8<sup>pos</sup> T cells. (B) *Ex vivo* IFN- $\gamma$  production by Melan-A-specific T cells following analog (n = 15) or natural (n = 9) peptide vaccination using Elispot assays. PBMCs were stimulated with the natural peptide (10  $\mu$ g/ml) for 16 hours and data were calculated as percentage of primed multimer<sup>pos</sup> CD8<sup>pos</sup> T cells. \*\*\* P < 0.001 (two-tailed unpaired *t* test). (C) Tumor cell killing was assessed by using T2 target cells (A2<sup>pos</sup>/TAP<sup>neg/neg</sup>) pulsed with graded concentration of the natural Melan-A peptide. Melan-A-specific T cell clones (n = 265) were generated *in vitro* following sorting of multimer<sup>pos</sup> EM28<sup>pos</sup> or EM28<sup>neg</sup> T cell subsets from melanoma patients who had been vaccinated with analog/ELA (n = 2) or natural/EAA (n = 2) peptide. Complete set of data representing maximal lysis. \*\*\* P < 0.001; ns, not significant (two-tailed unpaired *t* test). (D and E) Direct *ex vivo* cumulative expression of memory/homing and effector genes. Single tumor- and virus-specific EM28<sup>pos</sup> and EM28<sup>neg</sup>/EMRA T cells were sorted directly *ex vivo* from four patients vaccinated either with the analog/ELA (n = 2) or the natural/EAA (n = 2) peptide, as well as from two healthy donors with EBV- and CMV-specific T cell responses, and processed for cDNA<sup>plus</sup> amplification as described in Materials and Methods. Expression of (D) memory/homing-associated genes (*CD27*, *IL7R*, *EOMES*, *CXCR3* and *CCR5*) and (E) effector-associated genes (*IFNG*, *KLRD1*, *PRF1*, and *GZMB*) was determined for each individual cDNA<sup>plus</sup> cell. EM28<sup>pos</sup> (n = 398) and EM28<sup>neg</sup>/EMRA (n = 412) tested single-cell samples. \*\*\* 0.0001 < P < 0.001; \*\* 0.001 < P < 0.01; \* 0.01 < P < 0.1; ns, not significant (by one-way ANOVA test).

**Figure 5.** Heterogeneity and co-expression of memory/homing and effector genes by tumor- and virus-specific T cells. Polyfunctional gene expression profile was determined as a measure of co-expression of the five memory/homing-associated gene transcripts (*CD27*, *IL7R*, *EOMES*, *CXCR3* and *CCR5*) and the four effector-associated gene transcripts (*IFNG*, *KLRD1*, *PRF1*, and *GZMB*) within early-differentiated EM28<sup>pos</sup> (A) and late-differentiated EM28<sup>neg</sup>/EMRA (B) subsets. Colors of the pie arcs depict the co-expression of individual memory/homing or effector genes, while the color in the pie depicts the number of co-expressed memory/homing- or effector-associated genes, as determined by SPICE 5.2. Increased polyfunctional gene co-expression (from 0 up to 4 or 5) is shown as progressive color gradients. (A) EM28<sup>pos</sup> (n = 398) and (B) EM28<sup>neg</sup>/EMRA (n = 412) tested single-cell samples. ELA, analog peptide vaccination; EAA, natural peptide vaccination. P-values of the permutation test are shown in the figure below to the corresponding pies.

**Figure 6.** Direct *ex vivo* distribution of individual T cells according to combined simultaneous co-expression of memory/homing- and effector-associated gene transcripts. Memory/homing and effector- gene co-expression frequencies were determined for each single-cell (n = 810) and in all possible combinations using a three-dimensional matrix. X-axis, 0 to 5 memory/homing gene co-expression (M0 to M5 shown as progressive blue gradients; among *IL7R*, *CD27*, *EOMES*, *CXCR3*, and *CCR5*) versus z-axis, 0 to 4 effector gene co-expression (E0 to E4 shown as progressive red gradients; among *IFNG*, *KLRD1*, *PRF1* and *GZMB*) versus single-cell frequency (y-axis). Distribution of memory/homing and effector gene co-expression patterns from (A) single EM28<sup>pos</sup> and EM28<sup>neg</sup> T cells sorted after analog

(n = 2) or natural (n = 2) peptide vaccination (four patients), and (B) from single EM28<sup>pos</sup> and EMRA T cells sorted from EBV- and CMV-specific T cells (from healthy donors BCL6 and BCL8).

**Figure 7.** Heterogeneity and co-expression of memory/homing and effector gene patterns within dominant T cell clonotypes. Clonotypes were defined as dominant, when their relative frequencies within antigen-specific T cell subsets were found > 10%.<sup>24</sup> Analysis was performed on dominant T cell clonotypes that were shared between EM28<sup>pos</sup> and EM28<sup>neg</sup>/EMRA T cell subsets (selected with differentiation), as well as on dominant clonotypes that were exclusively found within the early-differentiated EM28<sup>pos</sup> subset (not selected with differentiation). The proportion within EM28<sup>pos</sup> and EM28<sup>neg</sup>/EMRA T cell subsets is depicted for each T cell clonotype. Gene co-expression patterns were determined on the five memory/homing- (*CD27*, *IL7R*, *EOMES*, *CXCR3* and *CCR5*) and the four effector- (*IFNG*, *KLRD1*, *PRF1*, and *GZMB*) associated gene transcripts within (A) early-differentiated EM28<sup>pos</sup> and (B) late-differentiated EM28<sup>neg</sup>/EMRA subsets using SPICE 5.2. Colors of the pie arcs depict the direct *ex vivo* co-expression of individual memory/homing or effector genes, while the color in the pie depicts the number of co-expressed memory/homing- or effector-associated genes. Increased polyfunctional gene co-expression (from 0 up to 4 or 5) is shown as progressive color gradients. (A, B) ELA; analog peptide vaccination. EAA; natural peptide vaccination. n.a; not applicable. EM28<sup>pos</sup> (n = 143) and EM28<sup>neg</sup>/EMRA (n = 112) tested single-cell samples.

## REFERENCES

1. Wiesel M, Walton S, Richter K, et al. Virus-specific CD8 T cells: activation, differentiation and memory formation. *APMIS*. 2009;117: 356-381.
2. Rutishauser RL and Kaech SM. Generating diversity: transcriptional regulation of effector and memory CD8 T-cell differentiation. *Immunol Rev*. 2010;235: 219-233.
3. Obar JJ and Lefrancois L. Memory CD8+ T cell differentiation. *Ann N Y Acad Sci*. 2010;1183: 251-266.
4. Willinger T, Freeman T, Hasegawa H, et al. Molecular signatures distinguish human central memory from effector memory CD8 T cell subsets. *J Immunol*. 2005;175: 5895-5903.
5. Holmes S, He M, Xu T, et al. Memory T cells have gene expression patterns intermediate between naive and effector. *Proc Natl Acad Sci U S A*. 2005;102: 5519-5523.
6. Fann M, Chiu WK, Wood WH, 3rd, et al. Gene expression characteristics of CD28null memory phenotype CD8+ T cells and its implication in T-cell aging. *Immunol Rev*. 2005;205: 190-206.
7. Kaech SM, Hemby S, Kersh E, et al. Molecular and functional profiling of memory CD8 T cell differentiation. *Cell*. 2002;111: 837-851.
8. Sarkar S, Kalia V, Haining WN, et al. Functional and genomic profiling of effector CD8 T cell subsets with distinct memory fates. *J Exp Med*. 2008;205: 625-640.
9. Appay V, Bosio A, Lokan S, et al. Sensitive gene expression profiling of human T cell subsets reveals parallel post-thymic differentiation for CD4+ and CD8+ lineages. *J Immunol*. 2007;179: 7406-7414.

10. Wherry EJ, Ha SJ, Kaech SM, et al. Molecular signature of CD8<sup>+</sup> T cell exhaustion during chronic viral infection. *Immunity*. 2007;27: 670-684.
11. Baitsch L, Baumgaertner P, Devevre E, et al. Exhaustion of tumor-specific CD8 T cells in metastases from melanoma patients. *J Clin Invest*. 2011;121: 2350-2360.
12. Levsky JM and Singer RH. Gene expression and the myth of the average cell. *Trends Cell Biol*. 2003;13: 4-6.
13. Levsky JM, Shenoy SM, Pezo RC, et al. Single-cell gene expression profiling. *Science*. 2002;297: 836-840.
14. Toriello NM, Douglas ES, Thaitrong N, et al. Integrated microfluidic bioprocessor for single-cell gene expression analysis. *Proc Natl Acad Sci U S A*. 2008;105: 20173-20178.
15. Liu X, Long F, Peng H, et al. Analysis of cell fate from single-cell gene expression profiles in *C. elegans*. *Cell*. 2009;139: 623-633.
16. Guo G, Huss M, Tong GQ, et al. Resolution of cell fate decisions revealed by single-cell gene expression analysis from zygote to blastocyst. *Dev Cell*. 2010;18: 675-685.
17. Peixoto A, Monteiro M, Rocha B, et al. Quantification of multiple gene expression in individual cells. *Genome Res*. 2004;14: 1938-1947.
18. Monteiro M, Evaristo C, Legrand A, et al. Cartography of gene expression in CD8 single cells: novel CCR7<sup>-</sup> subsets suggest differentiation independent of CD45RA expression. *Blood*. 2007;109: 2863-2870.
19. Iancu EM, Baumgaertner P, Wieckowski S, et al. Profile of a serial killer: cellular and molecular approaches to study individual cytotoxic T-cells following therapeutic vaccination. *J Biomed Biotechnol*. 2011;2011: 452606.

20. Flatz L, Roychoudhuri R, Honda M, et al. Single-cell gene-expression profiling reveals qualitatively distinct CD8 T cells elicited by different gene-based vaccines. *Proc Natl Acad Sci U S A*. 2011;108: 5724-5729.
21. Speiser DE, Baumgaertner P, Voelter V, et al. Unmodified self antigen triggers human CD8 T cells with stronger tumor reactivity than altered antigen. *Proc Natl Acad Sci U S A*. 2008;105: 3849-3854.
22. Bigouret V, Hoffmann T, Arlettaz L, et al. Monoclonal T-cell expansions in asymptomatic individuals and in patients with large granular leukemia consist of cytotoxic effector T cells expressing the activating CD94:NKG2C/E and NKD2D killer cell receptors. *Blood*. 2003;101: 3198-3204.
23. Rufer N, Reichenbach P and Romero P. Methods for the ex vivo characterization of human CD8+ T subsets based on gene expression and replicative history analysis. *Methods Mol Med*. 2005;109: 265-284.
24. Speiser DE, Wieckowski S, Gupta B, et al. Single cell analysis reveals similar functional competence of dominant and nondominant CD8 T-cell clonotypes. *Proc Natl Acad Sci U S A*. 2011;108: 15318-15323.
25. Speiser DE, Lienard D, Rufer N, et al. Rapid and strong human CD8+ T cell responses to vaccination with peptide, IFA, and CpG oligodeoxynucleotide 7909. *J Clin Invest*. 2005;115: 739-746.
26. Pittet MJ, Valmori D, Dunbar PR, et al. High frequencies of naive Melan-A/MART-1-specific CD8(+) T cells in a large proportion of human histocompatibility leukocyte antigen (HLA)-A2 individuals. *J Exp Med*. 1999;190: 705-715.
27. Brady G and Iscove NN. Construction of cDNA libraries from single cells. *Methods Enzymol*. 1993;225: 611-623.

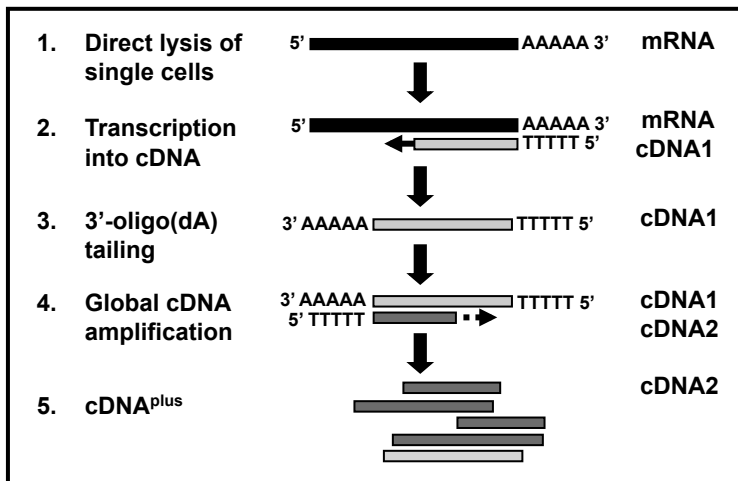
28. Sauvageau G, Lansdorp PM, Eaves CJ, et al. Differential expression of homeobox genes in functionally distinct CD34+ subpopulations of human bone marrow cells. *Proc Natl Acad Sci U S A*. 1994;91: 12223-12227.
29. Wieckowski S, Baumgaertner P, Corthesy P, et al. Fine structural variations of alphabetaTCRs selected by vaccination with natural versus altered self-antigen in melanoma patients. *J Immunol*. 2009;183: 5397-5406.
30. Iancu EM, Corthesy P, Baumgaertner P, et al. Clonotype selection and composition of human CD8 T cells specific for persistent herpes viruses varies with differentiation but is stable over time. *J Immunol*. 2009;183: 319-331.
31. Roux E, Dumont-Girard F, Starobinski M, et al. Recovery of immune reactivity after T-cell-depleted bone marrow transplantation depends on thymic activity. *Blood*. 2000;96: 2299-2303.
32. Sallusto F, Lenig D, Forster R, et al. Two subsets of memory T lymphocytes with distinct homing potentials and effector functions. *Nature*. 1999;401: 708-712.
33. Speiser DE, Baumgaertner P, Barbey C, et al. A novel approach to characterize clonality and differentiation of human melanoma-specific T cell responses: spontaneous priming and efficient boosting by vaccination. *J Immunol*. 2006;177: 1338-1348.
34. Romero P, Zippelius A, Kurth I, et al. Four functionally distinct populations of human effector-memory CD8+ T lymphocytes. *J Immunol*. 2007;178: 4112-4119.
35. Kobayashi N, Kondo T, Takata H, et al. Functional and phenotypic analysis of human memory CD8+ T cells expressing CXCR3. *J Leukoc Biol*. 2006;80: 320-329.

36. Appay V, van Lier RA, Sallusto F, et al. Phenotype and function of human T lymphocyte subsets: consensus and issues. *Cytometry A*. 2008;73: 975-983.
37. Kaech SM, Tan JT, Wherry EJ, et al. Selective expression of the interleukin 7 receptor identifies effector CD8 T cells that give rise to long-lived memory cells. *Nat Immunol*. 2003;4: 1191-1198.
38. Hamann D, Baars PA, Rep MH, et al. Phenotypic and functional separation of memory and effector human CD8+ T cells. *J Exp Med*. 1997;186: 1407-1418.
39. Intlekofer AM, Takemoto N, Wherry EJ, et al. Effector and memory CD8+ T cell fate coupled by T-bet and eomesodermin. *Nat Immunol*. 2005;6: 1236-1244.
40. Rufer N, Zippelius A, Batard P, et al. Ex vivo characterization of human CD8+ T subsets with distinct replicative history and partial effector functions. *Blood*. 2003;102: 1779-1787.
41. Derre L, Bruyninx M, Baumgaertner P, et al. In Vivo Persistence of Codominant Human CD8+ T Cell Clonotypes Is Not Limited by Replicative Senescence or Functional Alteration. *J Immunol*. 2007;179: 2368-2379.
42. Stahlberg A, Kubista M and Aman P. Single-cell gene-expression profiling and its potential diagnostic applications. *Expert Rev Mol Diagn*. 2011;11: 735-740.
43. Sul JY, Wu CW, Zeng F, et al. Transcriptome transfer produces a predictable cellular phenotype. *Proc Natl Acad Sci U S A*. 2009;106: 7624-7629.
44. Chubb JR, Treck T, Shenoy SM, et al. Transcriptional pulsing of a developmental gene. *Curr Biol*. 2006;16: 1018-1025.
45. Larsson C, Grundberg I, Soderberg O, et al. In situ detection and genotyping of individual mRNA molecules. *Nat Methods*. 2010;7: 395-397.
46. Bartfai T, Buckley PT and Eberwine J. Drug targets: single-cell transcriptomics hastens unbiased discovery. *Trends Pharmacol Sci*. 2012;33: 9-16.

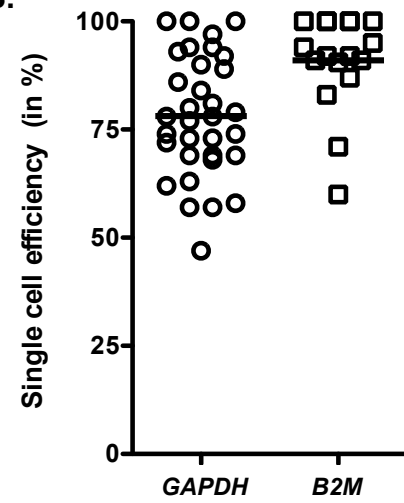
47. Hikono H, Kohlmeier JE, Takamura S, et al. Activation phenotype, rather than central- or effector-memory phenotype, predicts the recall efficacy of memory CD8<sup>+</sup> T cells. *J Exp Med*. 2007;204: 1625-1636.
48. Kohlmeier JE, Miller SC, Smith J, et al. The chemokine receptor CCR5 plays a key role in the early memory CD8<sup>+</sup> T cell response to respiratory virus infections. *Immunity*. 2008;29: 101-113.
49. Joshi NS, Cui W, Dominguez CX, et al. Increased numbers of preexisting memory CD8 T cells and decreased T-bet expression can restrain terminal differentiation of secondary effector and memory CD8 T cells. *J Immunol*. 2011;187: 4068-4076.
50. Chang JT, Ciocca ML, Kinjyo I, et al. Asymmetric proteasome segregation as a mechanism for unequal partitioning of the transcription factor T-bet during T lymphocyte division. *Immunity*. 2011;34: 492-504.
51. Stemberger C, Huster KM, Koffler M, et al. A single naive CD8<sup>+</sup> T cell precursor can develop into diverse effector and memory subsets. *Immunity*. 2007;27: 985-997.
52. Peixoto A, Evaristo C, Munitic I, et al. CD8 single-cell gene coexpression reveals three different effector types present at distinct phases of the immune response. *J Exp Med*. 2007;204: 1193-1205.
53. Betts MR and Harari A. Phenotype and function of protective T cell immune responses in HIV. *Curr Opin HIV AIDS*. 2008;3: 349-355.
54. Fonseca SG, Procopio FA, Goulet JP, et al. Unique features of memory T cells in HIV elite controllers: a systems biology perspective. *Curr Opin HIV AIDS*. 2011;6: 188-196.

55. Newell EW, Sigal N, Bendall SC, et al. Cytometry by Time-of-Flight Shows Combinatorial Cytokine Expression and Virus-Specific Cell Niches within a Continuum of CD8(+) T Cell Phenotypes. *Immunity*. 2012.
56. Haining WN and Barnitz RA. Deconvolving heterogeneity in the CD8+ T-cell response to HIV. *Curr Opin HIV AIDS*. 2012;7: 38-43.
57. Valmori D, Fonteneau JF, Lizana CM, et al. Enhanced generation of specific tumor-reactive CTL in vitro by selected Melan-A/MART-1 immunodominant peptide analogues. *J Immunol*. 1998;160: 1750-1758.
58. Cole DK, Edwards ES, Wynn KK, et al. Modification of MHC anchor residues generates heteroclitic peptides that alter TCR binding and T cell recognition. *J Immunol*. 2010;185: 2600-2610.
59. Stuge TB, Holmes SP, Saharan S, et al. Diversity and Recognition Efficiency of T Cell Responses to Cancer. *Plos Med*. 2004;1: e28.
60. Bioley G, Guillaume P, Luescher I, et al. Vaccination with a recombinant protein encoding the tumor-specific antigen NY-ESO-1 elicits an A2/157-165-specific CTL repertoire structurally distinct and of reduced tumor reactivity than that elicited by spontaneous immune responses to NY-ESO-1-expressing Tumors. *J Immunother*. 2009;32: 161-168.
61. Arden B, Clark SP, Kabelitz D, et al. Human T-cell receptor variable gene segment families. *Immunogenetics*. 1995;42: 455-500.

A.



B.



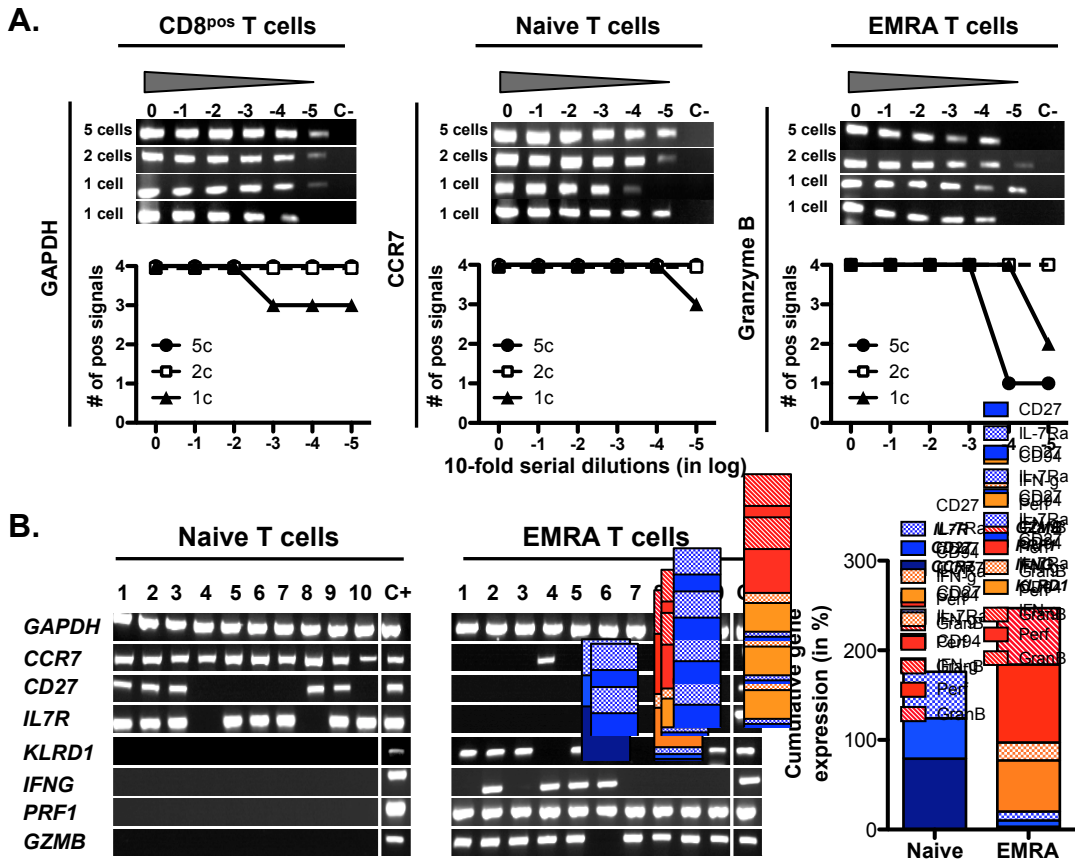


Figure 2

Gupta et al.

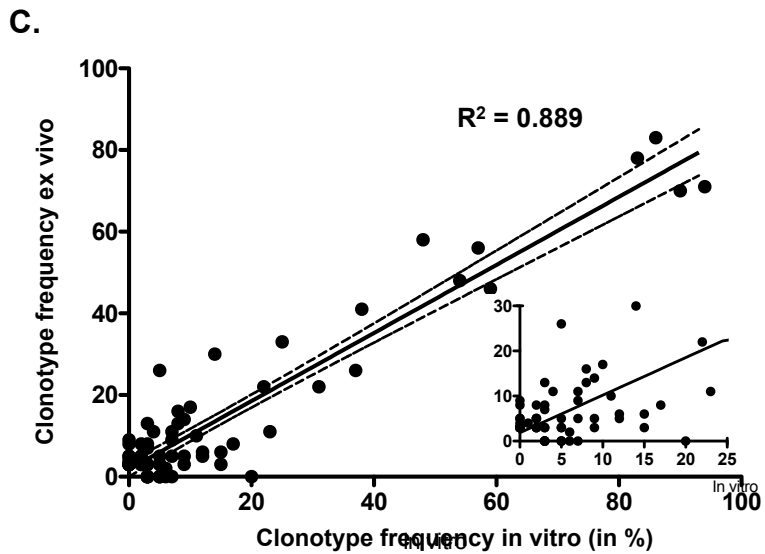
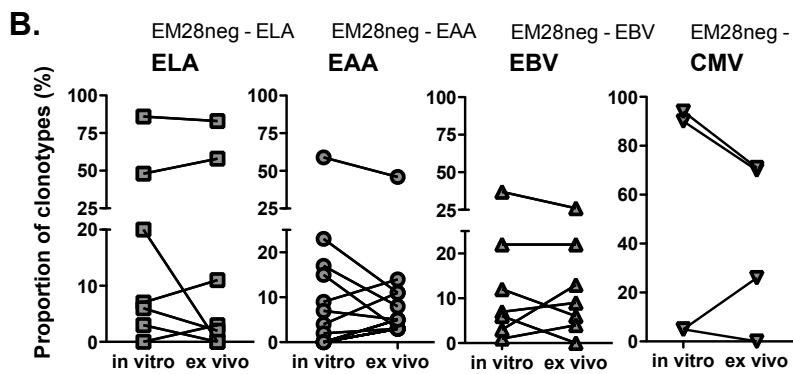
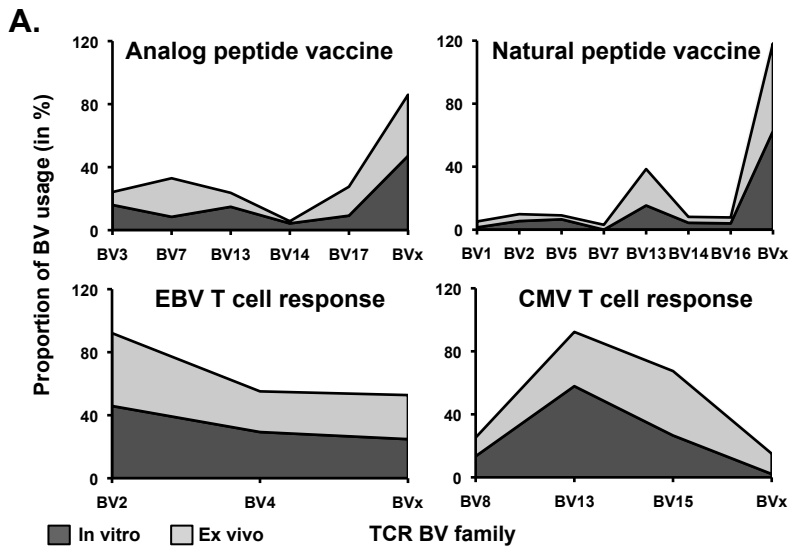


Figure 3

Gupta et al.

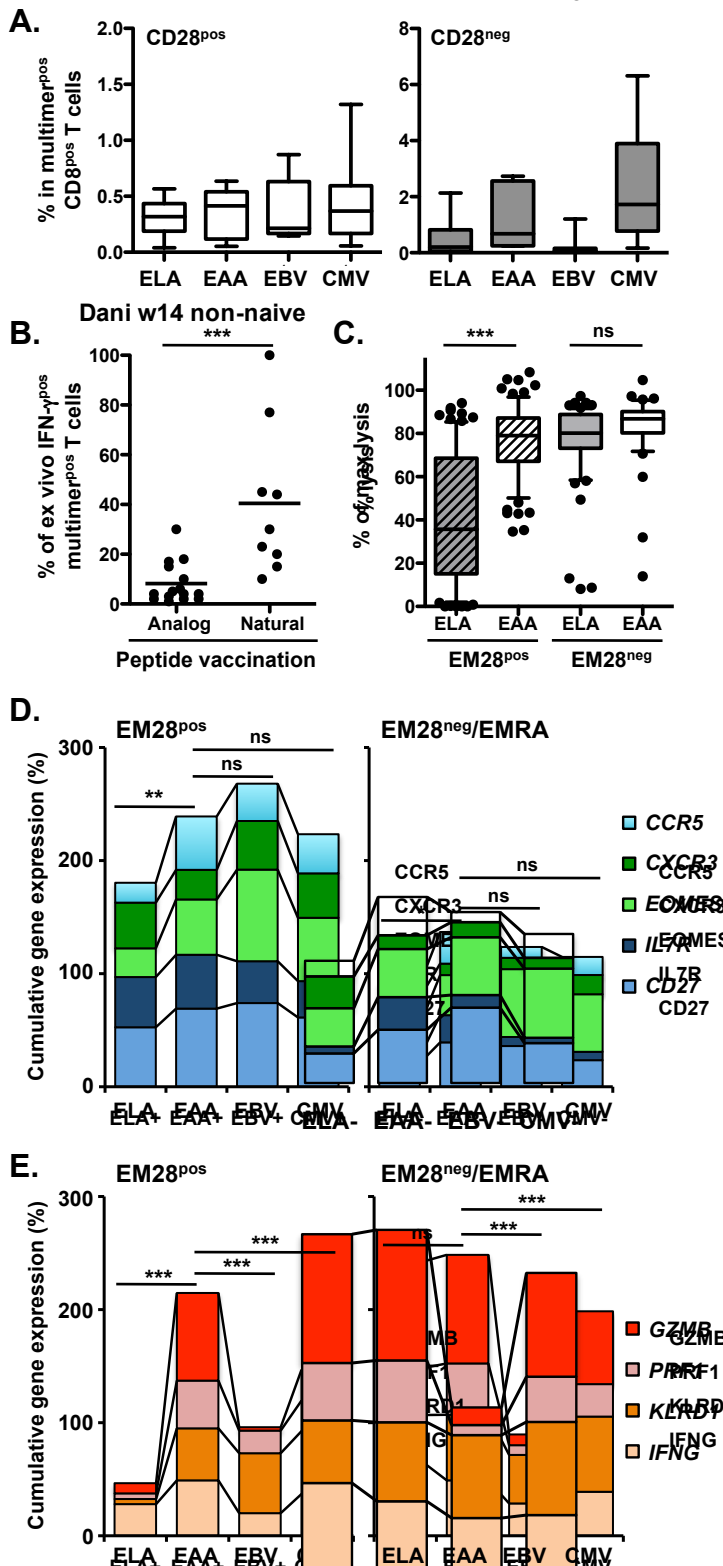


Figure 4

Gupta et al.

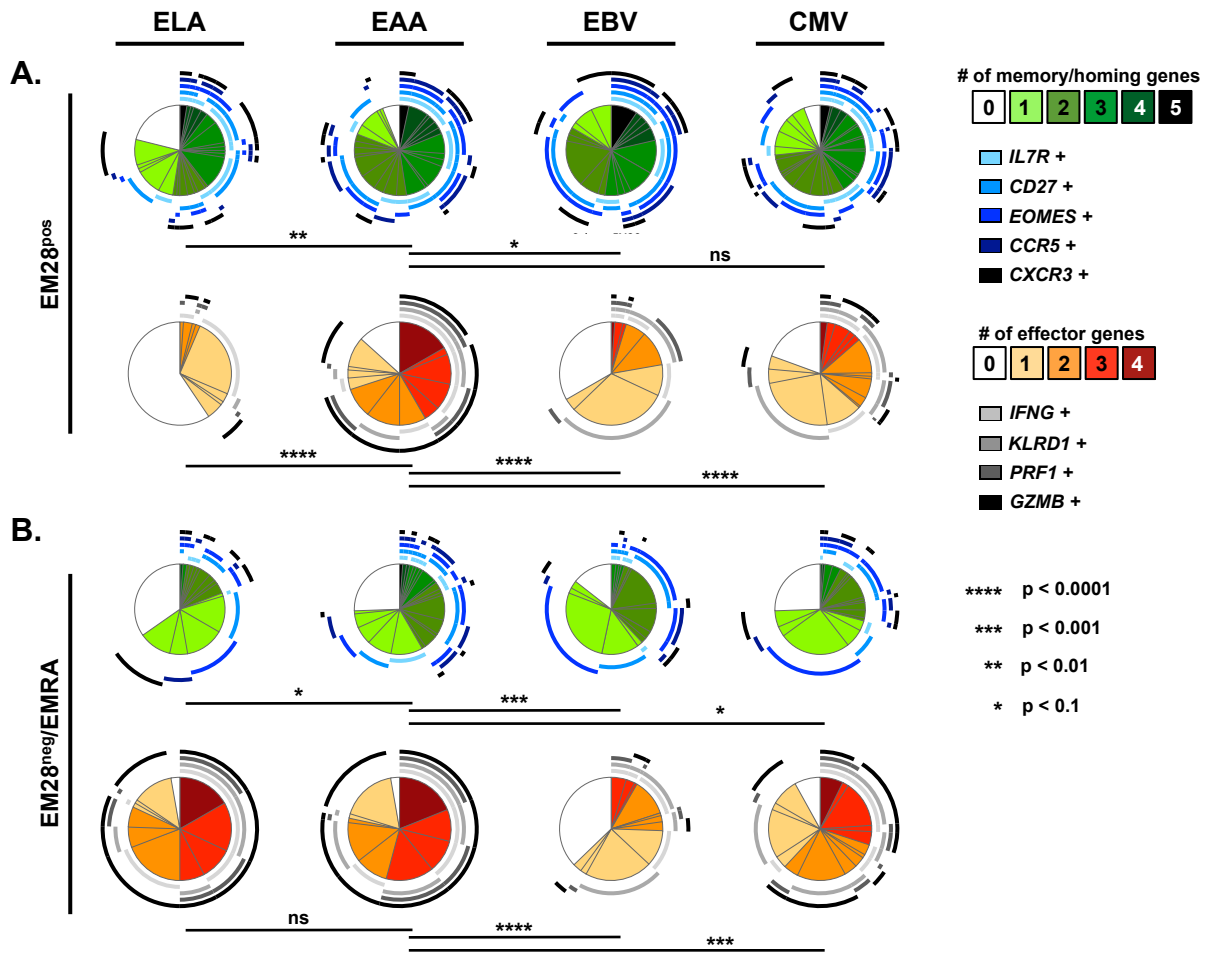


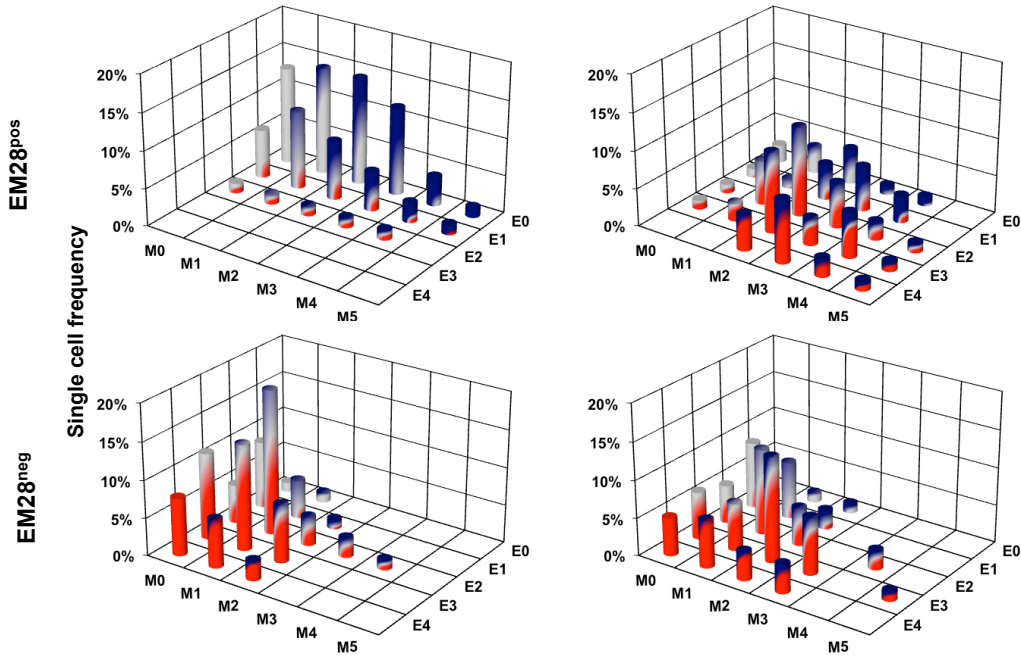
Figure 5

Gupta et al.

**A.**

**Analog peptide vaccine**

**Natural peptide vaccine**



**B.**

**EBV T-cell response**

**CMV T-cell response**

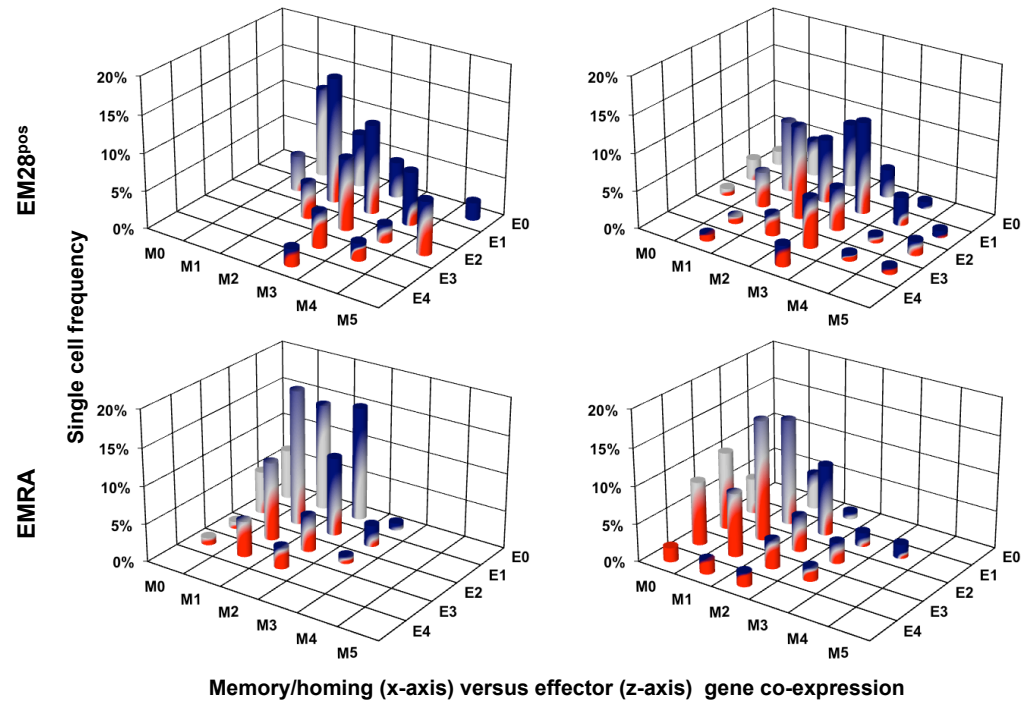


**Figure 6**

**Gupta et al.**

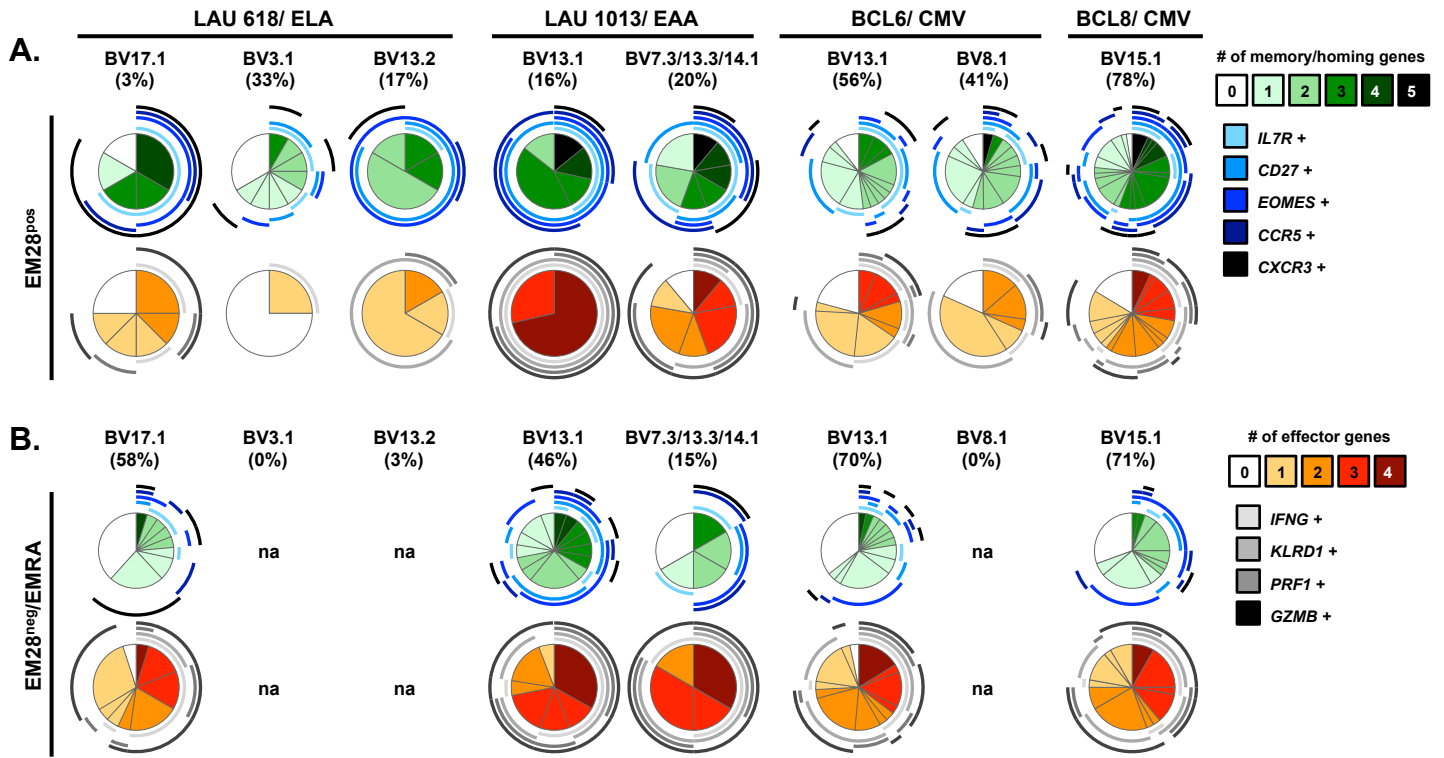


Figure 7

Gupta et al.